Weak Intramolecular Proton−Hydride and Proton−Fluoride Interactions: Experimental (NMR, X-ray) and DFT Studies of the Bis(NBH_3) and Bis(NBF_3) Adducts of 1,3-Dimethyl-1,3-diazolidine

Marisol Güizado-Rodríguez,[†] Armando Ariza-Castolo,[†] Gabriel Merino,[†] Alberto Vela,[†] Heinrich Noth,[‡] Vladimir I. Bakhmutov,*[,†] and Rosalinda Contreras*[,†]

Contribution from the Departamento de Química, Centro de Investigación y de Estudios Avanzados, A.P. 14-740, C.P. 07000, México D.F, México, and the Department of Chemistry, Ludwig-Maximilian University, Butenandt-Strasse 5-13 (Haus D), D-81377 Munchen, Germany

Received May 4, 2001. Revised Manuscript Received June 27, 2001

Abstract: Bis(NBH_3), bis(NBF_3), and NBF_3/NBH_3 adducts **1**−**3** were prepared from 1,3-dimethyl-1,3-diazolidine and characterized by the ^1H, ^{13}C, ^{11}B, ^{19}F, 2D $^1H-^{13}C$ HETCOR and NOESY NMR spectra. The structures and conformations of the adducts were established by the variable-temperature ^1H NMR spectra, the X-ray diffraction method (adduct **2A**), and density functional calculations at different theoretical levels. The experimental and theoretical data have revealed that bis adducts **1-3** prefer trans orientations of the borane groups (**1A**, **2A**, **3A**) in solution, the solid state, and the gas phase. The studies have shown that the energetic preference of trans adducts with respect to cis compounds, decreasing as **2A** (2.9 kcal/mol) > **3A** (2.7 kcal/mol) > **1A** (1.4 kcal/mol), is dictated by spatially repulsive interactions between the CH_3, BH_3, and BF_3 groups. The results of DFT calculations agree well with an experimental trans/cis isomeric ratio of 9:1 determined in solutions of adduct **1**. The calculated geometry and energy, as well as the topological analysis of electronic densities, show that trans adducts **1-3** should exist in gas phase as twist conformations **T-2** stabilized by the intramolecular $C-H^{\delta+}\cdots{}^{-\delta}H-B$ or $C-H^{\delta+}\cdots{}^{-\delta}F-B$ interactions. These interactions are characterized as closed-shell. The energy of one proton−hydride and proton−fluoride intramolecular contact, estimated as 1.9 (**1A**−**T-2**) and 0.7 (**2A**−**T-2**) kcal/mol, respectively, classifies the "elongated" intramolecular interactions $CH^{\delta+}\cdots{}^{-\delta}HB$ and $CH^{\delta+}\cdots{}^{-\delta}FB$ as weak ones. It has been established that, on going from gas phase to a condensed phase (solution and solid), the twist-conformations **T-2** transform to conformations **T-1**, probably by intermolecular dipole−dipole interactions. The data presented in this work show that despite a weakness of the "elongated" proton−hydride and proton−fluoride interactions, they can play a significant role in the stabilization of conformational molecular states, especially when cooperativity is in action.

Introduction

Proton−hydride ($H^{\delta+}\cdots{}^{-\delta}H$) interactions have attracted a great deal of the attention of chemists in the past few years.[1−4] These interactions result in the formation of the unusual intra- or intermolecular dihydrogen bonds. These bonds show a medium strength, $-\Delta H°$, ranging from 4 to 7 kcal/mol when negatively polarized H atoms in transition metal or amineborane hydrides act as proton acceptors.[1b,e,2b] The $H^{\delta+}\cdots{}^{-\delta}H$ bonding results in interatomic distances (1.75 to 1.9 Å)[2c,d] significantly less than the sum of the van der Waals radii of H. Intramolecular H−H distances can be even shorter. For example, the complex (η^5-$C_5H_4(CH_2)_3NMe_2H^+$)RuH(dppm) has a proton−hydride separation of 1.52 Å.[3a,b] Finally, the dihydrogen bonds play an important role in proton-transfer reactions to give dihydrogen complexes.[1b,d,e]

One can consider that shorter H−H distances indicate stronger interactions. Actually, ab initio calculations[3c−f] predict significant bond energies at short $H^{\delta+}\cdots{}^{-\delta}H$ distances. For example, the theoretically calculated H-bonded complexes LiH···HF and $H_3SiH\cdots HNH_3^+$ with $r(H\cdots H) = 1.60$ Å show $-\Delta H°$ of 10.9 and 5.0 kcal/mol, respectively. However, energies decrease dramatically, when $H^{\delta+}$ and $^{-\delta}H$ are separated by >2.0 Å

* Phone: + 52-5/747-38-00, ext. 4012. Fax: + 52-5/747-71-13. E-mail: vladimir@mail.cinvestav.mx and rcontrer@mail.cinvestav.mx.

[†] Centro de Investigación y de Estudios Avanzados.

[‡] Ludwig-Maximilian University.

(1) (a) Richardson, T. B.; de Gala, S.; Crabtree, R. H.; Siegbahn, P. E. M. *J. Am. Chem. Soc.* **1995**, *117*, 12875. (b) Shubina, E. S.; Belkova, N. V.; Krylov, A. N.; Vorontsov, E. V.; Epstein, L. M.; Gusev, D. G.; Niedermann, M.; Berke, H. *J. Am. Chem. Soc.* **1996**, *118*, 1105.(c) Peris, E.; Wessel, J.; Patel, B. P.; Crabtree, R. H. *J. Chem Soc., Chem. Commun.* **1995**, 2175. (d) Ayllón, J. A.; Gervaux, C.; Sabo-Etienne, S.; Chaudret B. *Organometallics* **1997**, *16*, 2000. (e) Shubina, E. S.; Belkova, N. V.; Bakhmutova, E. V.; Vorontsov, E. V.; Bakhmutov, V. I.; Ionidis, A. V.; Bianchini, C.; Marvelli, L.; Peruzzini, M.; Epstein, L. M. *Inorg. Chim. Acta* **1998**, *280*, 302.

(2) (a) Padilla-Martínez, I. I.; Rosalez-Hoz, M. J.; Contreras, R. 49th Southwest Regional ACS Meeting, October 24−27 1993. (b) Epstein, L. M.; Shubina, E. S.; Bakhmutova, E. V.; Saitkulova, L. N.; Bakhmutov, V. I.; Chistyakov, A. L.; Stankevich, I. V. *Inorg. Chem.* **1998**, *37*, 3013. (c) Klooster, W. T.; Koetzle, T. F.; Siegbahn, P. E. M.; Richardson, T. B.; Crabtree, R. H. *J. Am. Chem. Soc.* **1999**, *121*, 6337. (d) Crabtree, R. H.; Siegbahn, P. E. M.; Eisenstein, O.; Rheingold, A. C.; Koetzle, T. F. *Acc. Chem. Res.* **1996**, 348.

(3) (a) Ayllón, J. A.; Sayers, S. F.; Sabo-Etienne, S.; Donnadieu, B.; Chaudret, B.; Clot, E. *Organometallics* **1999**, *18*, 3981. (b) Matsubara, T. *Organometallics* **2001**, *20*, 19. (c) Grabowski, S. J. *J. Phys. Chem. A* **2000**, *104*, 5551. (d) Zhu, W. L.; Puah, C. M.; Tan, X. J.; Jiang, H. L.; Chen, K. X. *J. Phys. Chem. A* **2001**, *105*, 426. (e) Grabowski, S. J. *Chem. Phys. Lett.* **2000**, *327*, 203. (f) Calhorda, M. J. *Chem. Commun.* **2000**, 801.

(4) (a) Padilla-Martínez, I. I.; Rosales-Hoz, M. J.; Tlahuext H.; Camacho-Camacho, C.; Ariza-Castolo, A.; Contreras, R. *Chem. Ber.* **1996**, *129*, 441−449. (b) Flores-Parra, A.; Sánchez-Ruiz, S. A.; Guadarrama, C.; Nöth, H.; Contreras, R. *Eur. J. Inorg. Chem.* **1999**, 2069. (c) Güizado-Rodríguez, M.; Flores-Parra, A.; Sánchez-Ruiz, S. A.; Tapia-Benavides R.; Contreras, R.; Bakhmutov, V. I. *Inorg. Chem.* **2001**, *40* 3243.

10.1021/ja0111232 CCC: $20.00
Published on Web 08/23/2001

Chart 1

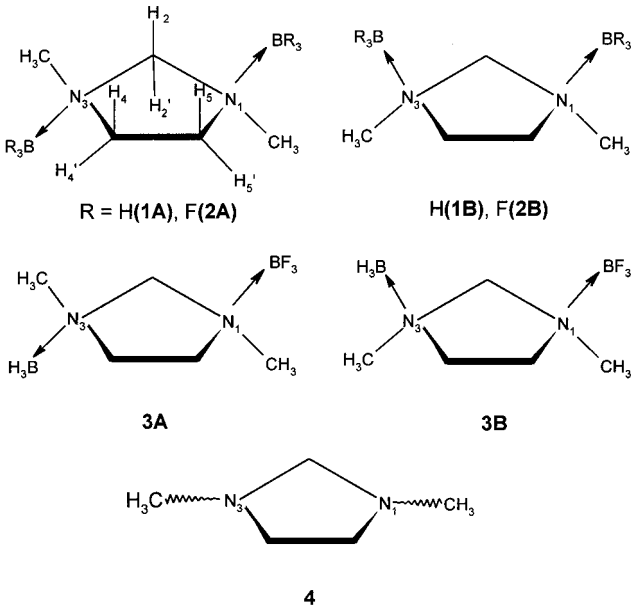

(-$\Delta H°$ < 0.9−0.4 kcal/mol). Intramolecular contacts C−$H^{\delta+}$•••$^{-\delta}$H−B, established for cyclic amineboranes in the solid state and solution, are remarkably elongated up to 2.2−2.5 Å.[4a−c] These H−H contacts could represent a lowest limit of weak interactions. Therefore, studies of their role in the structural features of molecular aggregates are of great interest.

Like the cyclic N−BH_3 amineboranes, their N−BF_3 derivatives reveal in solid-state contacts C−$H^{\delta+}$•••$^{-\delta}$F−B that are also less than the sum of the van der Waals radii of H and F.[4a,b] It has been found that stable N−B bonds in the borane adducts of five- or six-membered heterocycles "freeze" the ring and nitrogen inversion, leading to preferable conformations of the cycles.[5,6a] Formally, this effect can be attributed to a specific influence of BH_3 and BF_3,[4b,6] provoking interactions C−$H^{\delta+}$•••$^{-\delta}$H−B or C−$H^{\delta+}$•••$^{-\delta}$F−B, where the C−$H^{\delta+}$ component is an α-methylene proton (in the cycles). In addition, the presence of the BH_3 or BF_3 groups strongly modifies the ^{1}H NMR spectra of such systems, causing the significant chemical shifts of neighboring protons.[5,6]

To help clarify this problem, we have focused on NMR and X-ray studies and density functional theory (DFT) calculations[6c,d] of amine bis(boranes) **1**-**3** (Chart 1). These compounds are good models to study the influence of BH_3 and BF_3, as compared with the CH_3 group, on isomeric and conformational properties of these molecular systems.

Results

NMR Studies. Borane adducts **1**−**3**, prepared from 1,3-dimethyl-1,3-diazolidine (**4**), were characterized by the ^{1}H, ^{13}C, ^{11}B, ^{19}F (see Experimental Section) and 2D ^{1}H−^{13}C HETCOR NMR spectra, supporting structural formulations in Chart 1. The cyclic protons of **1**−**3** are diastereotopic in the ^{1}H NMR spectra and, thus, the N−B bonds are stable on the NMR time scale. The room temperature (RT) ^{11}B NMR spectra of the compounds show the well-resolved coupling ^{11}B−^{1}H and ^{11}B−^{19}F, corresponding to a moderate ^{11}B relaxation rate. Hence, a ^{11}B−^{1}H coupling through three chemical bonds may affect the ^{1}H line widths, helping in the spectral assignments.

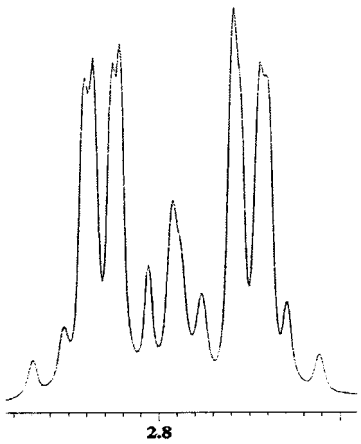

Figure 1. AA′BB′ pattern of protons 5(4′) and 5′(4) in the room temperature ^{1}H NMR spectrum of a C_6D_6 solution of trans diborane adduct **1A**.

Isomerism and conformational behavior of the compounds can be deduced from the NMR data. We have found that a treatment of **4** with 2 equiv of BH_3·$S(CH_3)_2$ results in isomeric adducts **1A** and **1B** in a ratio of 9:1.[6b] The RT ^{1}H NMR spectrum of the major adduct (**1A**) in $CDCl_3$ unexpectedly shows three singlet lines (Experimental Section) that correspond to equivalent protons 2, 2′ (4.08 ppm) and 5, 5′, 4, 4′ (3.57 ppm) and CH_3N(1), CH_3N(3). However, in C_6D_6, the N(1)CH_2-CH_2N(3) resonance transforms to a complicated pattern (Figure 1), but protons 2 and 2′ remain equivalent.

This pattern can be assigned to chemically nonequivalent protons 5 and 5′ (or 4′ and 4, respectively) in trans bis(borane) adduct **1A**. To be sure that the central "triplet" component of the pattern is indeed a feature of a spin system, but not an impurity signal, we have measured ^{1}H−T_1 relaxation times. The side lines of the multiplet showed T_1 values between 3.55 and 3.29 s, whereas the central component had a slightly smaller T_1 value (2.75 s). Note that such relaxation behavior is typical of a strongly coupled spin system undergoing the so-called coupled relaxation.[7]

Simulation procedures for the AA′BB′ pattern lead to results that are summarized in Table 1. It is important to note that the multiplet can be calculated when it is assumed that the geminal ^{1}H, ^{1}H couplings are negative[8a] and the J(5−4′) and J(5′-4) constants take different but positive values: 9.5 and 2.5 Hz, respectively. As a result of properties of the AA′BB′ spin system, the values can be interchanged. Nevertheless, these constants are very typical of the "frozen" conformations of cyclohexanes and their derivatives.[8b]

The NOESY ^{1}H NMR spectra of **1A** in C_6D_6 (25 °C) or toluene-d_8 (25° and −90 °C) revealed cross peaks 2(2′)-CH_3, 5′(4)-CH_3 and 5−5′ and provided the correct assignments, reported in Table 1. It is also worth mentioning that ^{1}H NMR spectra, recorded in a toluene solution, were temperature-

(5) (a) Flores-Parra, A.; Farfán, N.; Hernández-Bautista, A. I.; Fernández-Sánchez, L.; Contreras, R. *Tetrahedron* **1991**, *47*, 6903. (b) Contreras, R.; Santiesteban, F.; Paz-Sandoval, M. A.; Wrackmeyer, B. *Tetrahedron* **1984**, *40*, 3829. (c) Paz-Sandoval, M. A.; Santiesteban, F.; Contreras, R. *Magn. Reson. Chem.* **1985**, *23*, 428.

(6) (a) Flores-Parra, A.; Cadenas-Pliego, G.; Martínez-Aguilera, L. M. R.; García-Nares, M. L.; Contreras, R.; *Chem. Ber.* **1993**, *126*, 863. (b) Ariza-Castolo, A.; Contreras, R. in *Current Topics in the Chemistry of Boron*, Kabalka, G. W., Ed.; 1994, p 90. (c) Muller-Dethlefs K.; Hobza P. *Chem. Rev.* **2000**, *100*, 143−167. (d) Rappe A. K.; Bernstein E. R. *J. Phys. Chem. A* **2000**, *104*, 6117−6128.

(7) (a) Schaublin, S.; Hohener, A.; Ernst, R. R. *J. Magn. Reson.* **1974**, *13*, 196. (b) Bakhmutov, V. I.; Vorontsov, E. V. *Inorg. Chem. Rev.* **1998**, *18*, 183.

(8) (a) Gunter, H. *NMR Spectroscopy*, 2nd ed.; Wiley and Sons: New York, 1995; p 109. (b) Anderson, J. E.; Cai, J.; Davies, A. G. *J. Chem. Soc., Perkin. Trans.2*. **1997**, 2633.

Table 1. RT ^{1}H NMR Spectra (δ (ppm), J (Hz)) of **1A**, **1B**, and **2A** in $CDCl_3$

adduct	$\delta(CH_2)$	^2J(HCH)	^3J(HCCH)
1[a]	3.57 (2, 2′),[b] 2.84 (5, 4′),[b] 2.77 (5′, 4)[b]	−10.5 (4−4′),[b] −10.5 (5−5′)[b]	9.5 (5−4′),[b] 2.5 (5′−4),[b] 6.5 (5−4),[b] 6.5 (5′−4′)[b]
1B	4.41 (2),[c] 3.85 (2′), 3.75 (5, 4), 3.35 (5′,4′)	−11 (2−2′),[d] −11 (4−4′, 5−5′)	7 (4−5, 4′−5′), 9 (4−5′, 4′−5)
2A	4.21 (2, 2′),[c] 3.82 (5, 4′),[c] 3.26 (5′, 4),[c]	−10−11 (4−4′), −10−11 (5−5′)	9−10 (5−4′), 2−3 (5′−4), 5−6 (5−4), 5−6 (5′−4′)

[a] For the assignments, see Chart 1. [b] In benzene-d_6. [c] Broadened due to ^{1}H−^{11}B couplings. [d] The spin system was not sensitive to the ^{2}J(HCH) sign and the negative sign is used by analogy with **1A**.

Chart 2

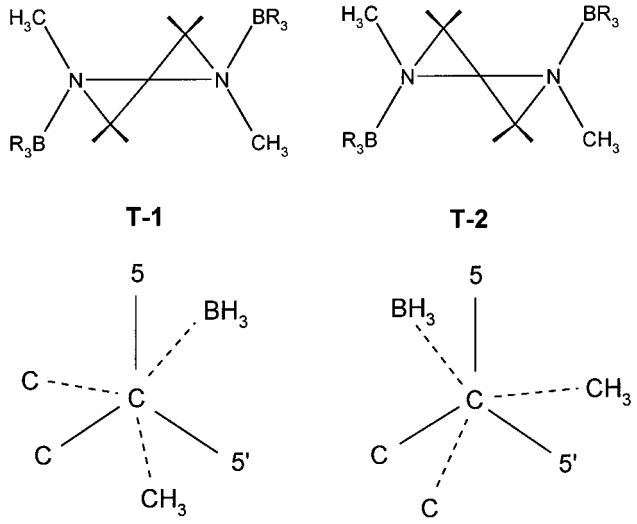

dependent; however, all the resonances showed the similar high-field displacements at low temperatures. Hence, adduct **1A** does not undergo conformational modifications in the temperature range between 25° and −90 °C. Finally, calculations of the 5(4′)−5′(4) patterns, observed at 25 °C and −90 °C, led to identical results: $^2J(5-5') = -10.5$ Hz, $^3J(5-4') = 9.5-10.0$ Hz, $^3J(5'\text{-}4) = 2.0-3.0$ Hz, $^3J(5-4) = 7.0$ Hz, $^3J(5'\text{-}4') = 7.0$ Hz, and $^2J(4-4') = -10.5$ Hz.

Similar spectral data were obtained for a $CDCl_3$ solution of the bis(BF_3) adduct **2A**. Note, however, that all of the signals of **2A** were strongly broadened in the RT ^{1}H NMR spectrum as a result of a pronounced three-bond ^{1}HCN^{11}B coupling. Therefore, the spectral simulations were performed using the ^{1}H{^{11}B} regime.

Protons 2 and 2′ can be chemically equivalent only for trans BH_3/BH_3 or BF_3/BF_3 arrangements. In agreement herewith, these protons remain as singlets in the ^{1}H NMR spectra of **1A** (toluene-d_8) and **2A** (CD_2Cl_2), recorded at −90 °C.

A cis BH_3/BH_3 arrangement in **1** should correspond to a chemical nonequivalence of protons 2 and 2′ and also 5(4) and 5′(4′). This is observed in the RT ^{1}H NMR spectrum of the minor isomer, even in $CDCl_3$ (Table 1); hence, the minor isomer can indeed be formulated as **1B**. Finally, in contrast to the bis-(BH_3) adduct, the NMR spectra of the bis(BF_3) (**2B**) and BH_3/BF_3 (**3B**) adducts did not reveal the presence of cis isomers.

Five-membered cycles undergo usually fast pseudorotation, leading to the equilibrated envelope (E) and twist (T) conformations in solution.[9] However, the modified Karplus equation,[10a] applied to the J(5−4′) and J(5′−4) constants in **1A** and **2A**, reveals a significant preference of only one conformation, where

(9) (a) Pfafferott, G.; Oberhammer, H.; Boggs, J. E.; Caminati, W. *J. Am. Chem. Soc.* **1985**, *107*, 2305. (b) Pfafferott, G.; Oberhammer, H.; Boggs, J. E. *J. Am. Chem. Soc.* **1985**, *107*, 2309. (c) Rockenbauer, A.; Korecz, L.; Hideg, K. *J. Chem. Soc., Perkin. Trans. 2* **1993**, 2149.

(10) (a) Haasnoot, C. A. G.; de Leeuw, F. A. A. M.; Altona, C. *Tetrahedron* **1980**, *36*, 2783. (b) Khan, M. A.; Peppe, C.; Tuck, D. G. *Can. J. Chem*. **1984**, *62*, 1662.

Table 2. X-ray Intramolecular B−F$^{\delta-}\cdots^{\delta+}$H−C Distances in Adduct **2A**[a]

distance	X-ray, Å
1	2.431
2	2.456
5	2.482
6	2.448
7	2.518
8	2.476

[a] See Figure 2A.

the corresponding dihedral angles differ strongly. The X-ray diffraction structure of **2A** in the crystal (see below) showed a twist conformation (**T-1** in Chart 2) with dihedral angles 5−4′, 5−4, 5′−4 and 5′−4′ of 169, 42, 87, and 40°, respectively.

For such arrangements of the protons, the modified Karplus equation predicts the ^3J(H−H) constants of 10.6, 6.8, 2.0, and 7.0 Hz, respectively. Good agreement with the experimental data allows us to suggest that only the states corresponding to conformations **T-1** are significantly populated in solutions of both adducts, even at room temperature. Additionally, cross peaks 5′(4)−CH_3 in the NOESY spectra support only **T-1**, because for **T-2**, one should expect the appearance of cross peaks 5′(4)−CH_3 as well as 5(4′)−CH_3. As mentioned above, all of the signals in the RT ^{1}H NMR spectrum of **2A** ($CDCl_3$) are broadened because of the ^{1}HCN−^{11}B coupling. It is interesting that this broadening effect is more pronounced for the resonance of H2, 2′ ($\Delta\nu = 6.7$ Hz versus 2.1 Hz, detected for the CH_3 line). This observation is not in conflict with the existence of **T-1**, where by analogy with Karplus's rule, protons 2 and 2′ are coupled by two ^{11}B nuclei with dihedral angles 2(2′)−C−N^{11}B close to 0° (13° from the X-ray data). Finally, the twist conformations are well-supported by the small values of the vicinal couplings of protons 5′ and 4, because the electronegative nitrogen atoms are located trans to one of the CH bonds.

Additional structural information can be obtained by ^{1}H−T_1 relaxation measurements in solution.[4c] The methylene protons in solid **2A** have short intramolecular contacts CH$^{\delta+}\cdots^{-\delta}$FB (see Table 2). The dipole−dipole proton−fluorine interactions could reduce T_1 times of the methylene protons, which are closer to BF_3. However, all of the ring protons showed the practically identical T_1 times in $CDCl_3$ at 25° C: 2.56 s(2, 2′), 2.53 (5, 4′), and 2.38 s (5′, 4). Note that the T_1 difference between protons 5 and 5′ is very close to errors in T_1 determinations (5%). The same results are obtained for **1A** in $CDCl_3$, where protons 2, 2′and 5, 5′ and 4, 4′ exhibit the T_1 values of 2.90 and 2.55 s, respectively. One can conclude that the diastereotopic methylene protons in conformations **T-1** are subject to strong dipolar interactions with BR_3 and CH_3. Similar dipolar interactions should be expected for the NCH_3 protons, neighbored to BR_3. These CH$^{\delta+}\cdots^{-\delta}$FB contacts are also short in solid **2A** (2.4−2.5 Å, Table 2). In full accord, the mono N(1)BH_3 and N(1)-BF_3 adducts, prepared from **4**,[6b] have shown that the CH_3N(1) protons relax remarkably faster with respect to CH_3(N3): 2.01 s versus 2.57 s in the BH_3 monoadduct and 2.51 s versus 3.43 s in the BF_3 mono adduct ($CDCl_3$, 25 °C).

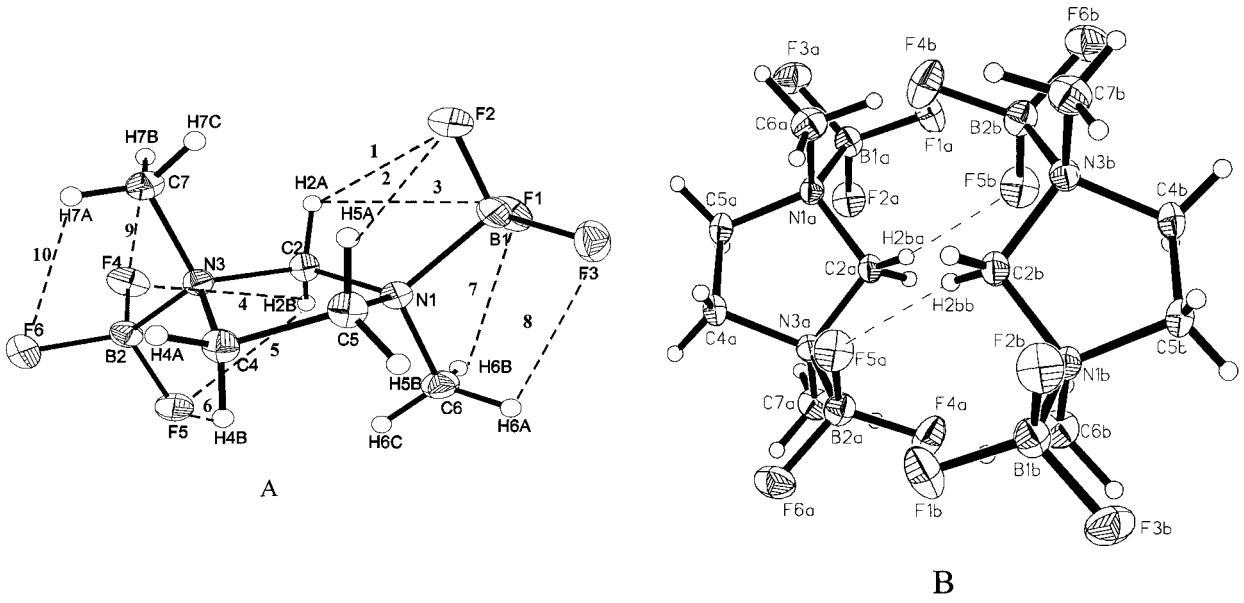

Figure 2. X-ray structure of bis(BF_3) adduct **2A**.

Inspection of the ^{1}H NMR data, reported in Table 1 and the Experimental Section, reveals the spectral effects of BH_3 and BF_3. Comparison of **4** and **1A** ($CDCl_3$) shows resonance 2, 2′ to be high-frequency-shifted by 0.5 ppm because of the influence of one cis BH_3 group. Two BH_3 groups (compare **4** and **1B**) act reasonably stronger (0.83 ppm). The parameters of the adducts containing the BH_3 and BF_3 groups demonstrate the more pronounced influence of BF_3 with respect to BH_3: 0.63 versus 0.5 ppm. Similar effects caused by the presence of BH_3 have already been reported for six-membered borane cyclic adducts.[5b,c] Note, however, that the strong chemical nonequivalence of the axial and equatorial protons is often observed in frozen conformations of cyclohexanes, even in the absence of BH_3 or BF_3, and the chemical shift differences can reach 1.5 ppm as a result of the electronic influence of neighboring groups.[8b]

The X-ray Structure of Adduct 2A. Among the investigated compounds, adduct **2A** was obtained as single crystals suitable for an X-ray analysis. Relevant data are presented in Figure 2, Table 2, and Tables 1SM and 2SM of the Supporting Information.

The compound is crystallized as a *R,R* and *S,S* pair of the trans forms. It is interesting that the pair is separated in the crystalline lattice by the short intermolecular distance of 2.48 Å between the BF_3 and C(2)H groups (Figure 2B). Intramolecular contacts $B-F^{\delta-}\cdots^{\delta+}H-C$ are also shortened (Table 2, Figure 2A), probably causing the following angular deformations: F1−B1−N1 = 106.70(13)°, F2−B1−N1 = 107.11(12)°, F3−B1−N1 = 106.05(13)°, F4−B2−N3 = 106.64(12)°, F5−B2−N3 = 106.89(12)°, and F6−B2−N3 = 106.08(15)°. Finally, structure **2A** shows a twist conformation, **T-1**, suggested above on the basis of the solution NMR data. The corresponding torsion angles, describing **T-1** as truly a twist conformation, are determined as 31.9° (C(2)−N(1)−C(5)−C(4)), −12.3° (C(5)−N(1)−C(2)−N(3)), 31.9° (C(2)−N(3)−C(4)−C(5)) and −12.3° (C(4)−N(3)−C(2)−N(1)). Add that in contrast to **2A**, its methyl analogue, 1,1,3,3-tetramethylimidazolidinium dication, exists in the solid state as the usual envelope conformation;[10b] however, this conformation can be dictated by the anion influence.

DFT Calculations of Adducts 1−3. Dihydrogen and $CH^{\delta+}\cdots^{-\delta}FB$ bonds can be identified by theoretical methods.[3c] Actually, experimental approaches, such as common X-ray, neutron diffraction in solid state, or NMR relaxation in solution, can locate atomic nuclei but not chemical bonds. Note, in addition, that the topological analysis of the electron density, determined experimentally by X-ray diffraction, is objectively difficult. In recent years, the theoretical topological analysis of the electron density has been proven to be a valuable tool to explore the existence of weak inter- and intramolecular interactions.[11a,b] In this section, details of the DFT calculations of structures **1-3,** including geometry optimizations, conformational energy differences, and the topological analysis of their electron densities are presented.

Geometry of 1−3. Full geometry optimizations (no symmetry restrictions) of molecules **1**−**3** were performed with Gaussian[11c] using the Berny optimization algorithm. Every stationary point was characterized as a local minimum on the potential energy surface (PES) by a harmonic (frequency) analysis. To gain insight into the capability of DFT to properly describe the structure and energetics of the amineboranes studied in this work, and because the X-ray structure of **2A**−**T1** is available, this conformer was calculated using three different exchange-correlation energy functionals, E_{XC}, and with three different basis sets. The functionals tested were a local E_{XC} with the exchange of the uniform electron gas and the correlation of Vosko, Wilk, and Nusair (VWN);[12a] a generalized gradient approximation (GGA) with the exchange proposed by Becke[12b] (B) and the correlation from Lee, Yang, and Parr (LYP);[12c,d] and a hybrid functional available in Gaussian with B exchange and LYP

(11) (a) Bader, R. F. W. *Atoms in Molecules. A Quantum Theory*; Oxford University Press: New York, 1990. (b) Mallison, P. R.; Wozniak, K.; Smith, G. T.; McCormack, K. L. *J. Am. Chem. Soc.* **1997**, *119*, 11502. (c) Frisch, M. J.; Trucks, G. W.; Schlegel, H. B.; Scuseria, G. E.; Robb, M. A.; Cheeseman, J. R.; Zakrzewski, V. G.; Montgomery, J. A.; Stratmann, R. E.; Burant, J. C.; Dapprich, S.; Millam, J. M.; Daniels, A. D.; Kudin, K. N.; Strain, M. C.; Farkas, O.; Tomasi, J.; Barone, V.; Cossi, M.; Cammi, R.; Mennucci, B.; Pomelli, C.; Adamo, C.; Clifford, S.; Ochterski, J.; Petersson, G. A.; Ayala, P. Y.; Cui, Q.; Morokuma, K.; Malick, D. K.; Rabuck, A. D.; Raghavachari, K.; Foresman, J. B.; Cioslowski, J.; Ortiz, J. V.; Stefanov, B. B.; Liu, G.; Liashenko, A.; Piskorz, P. ;Komaromi, I.; Gomperts, R.; Martin, R. L.; Fox, D. J.; Keith, T.; Al-Laham, M. A.; Peng, C. Y.; Nanayakkara, A.; Gonzalez, C.; Challacombe, M.; Gill, P. M. W.; Johnson, B. G.; Chen, W.; Wong, M. W.; Andres, J. L.; Head-Gordon, M.; Replogle, E. S.; Pople, J. A. *Gaussian 98 Revision A.7*; Gaussian, Inc.: Pittsburgh, PA, 1998.

Table 3. Mean Absolute Errors (MAE) and Largest Deviations (LD) of Optimized Geometries of **2A**-T_1 from the Structural X-ray Data[a]

	LDA	BLYP	B3LYP
		Bond Distances	
MAE	0.062	0.053	0.052
LD	C(7)−H(7A)	C(7)−H(7A)	C(7)−H(7A)
	0.170	0.160	0.160
		Intramolecular Distances	
MAE	0.166	0.093	0.087
LD	F(5)−H(6C)	F(5)−H(6C)	F(5)−H(6C)
	0.646	0.384	0.358
		Bond Angles	
MAE	1.8	1.7	1.7
LD	H(6C)−C(6)−H(6A)	H(6C)−C(6)−H(6A)	H(6C)−C(6)−H(6A)
	8.60	9.40	8.60
		Dihedral Angles	
MAE	6.3	5.3	4.6
LD	C(7)−N(3)−C(2)−N(1)	C(7)−N(3)−C(2)−N(1)	B(2)−N(3)−C(2)−N(1)
	13.6	10.8	9.5

[a] Obtained with a local (LDA), generalized gradient approximation (BLYP) and a hybrid (B3lYP) exchange-correlation energy functionals. Distances are in angstroms and angles are in degrees. All optimizations were done with a DZVP basis set.

Table 4. Mean Absolute Errors (MAE) and Largest Deviations (LD) of Optimized Geometries of **2A**-T_1 from the Structural X-ray Data[a]

	DZVP	DZVP2	6-31+G(d,p)
		Bond Distances	
MAE	0.052	0.051	0.052
LD	C(7)−H(7A)	C(7)−H(7A)	C(7)−H(7A)
	0.159	0.159	0.160
		Intramolecular Distances	
MAE	0.087	0.087	0.103
LD	F(5)−H(6C)	F(5)−H(6C)	F(5)−H(6C)
	0.358	0.359	0.425
		Bond Angles	
MAE	1.7	1.6	1.7
LD	H(6C)−C(6)−H(6A)	H(6C)−C(6)−H(6A)	H(6C)−C(6)−H(6A)
	9.4	9.3	9.2
		Dihedral Angles	
MAE	4.6	4.5	5.3
LD	B(2)−N(3)−C(2)−N(1)	B(2)−N(3)−C(2)−N(1)	B(2)−N(3)−C(2)−N(1)
	9.5	9.3	10.9

[a] Obtained with a hybrid (B3LYP) exchange-correlation energy functional for different basis sets. Distances are in angstroms and angles are in degrees.

correlation.[12e] In the rest of this work, these exchange-correlation functionals will be denoted by LDA, BLYP and B3LYP, respectively. On the other hand, to study the role of the basis, the following sets were considered: a double-ζ basis without p-polarization functions in the hydrogen atoms and with d-polarization functions in the heavy atoms (DZVP),[12f] a double-ζ basis with polarization functions in all atoms (DZVP2),[12f] and the internal Gaussian basis set 6-31+G(d,p).[12a] The contractions of the DZVP basis set are (41) for hydrogen and (621/41/1*) for the heavy atoms. In the case of the DZVP2 basis, the contractions are (41/1*) for hydrogen and (721/51/1*) for the heavy atoms. The optimized structures are reported in Table 2SM (Supporting Information).

To analyze the influence of the E_{XC} functional on the computed geometry of these compounds, the mean absolute error (MAE) and largest deviations (LD) from the X-ray data are presented in Table 3. As it is seen, the smallest errors in all types of structural parameters are provided by the hybrid functional followed by the GGA.

Special attention deserves LD, obtained for the bond angles; all theoretical levels have an error of ∼8−9 degrees that can be attributed to the packing effect in the solid state. Taking the hybrid as a reference, the effect of the basis set is summarized in Table 4. It is worth noting that the selected basis sets allow us to study not only the role of p functions in hydrogen and diffuse functions in all atoms, but additionally, the effect of basis sets optimized within different theoretical methodologies, namely, DZVP and DZVP2 were optimized within LDA,[12f] but 6-31+G(d,p), in Hartree−Fock.[12a]

It follows from Table 4 that the smallest errors are obtained with the DZVP2 basis set followed by DZVP. The largest discrepancies correspond to the 6-31+G(d,p), but they are close to the LDA-optimized basis sets. Thus, from these results, one can conclude that the hybrid approach B3LYP with any of the basis used in this work is a reasonable chemical model to study the molecular structure of amineboranes.

It should be noted that, independent of the chemical model, the lowest lying conformers of **1A**, **2A**, and **3A** are the twist structures **T-2**. This result does not correspond to the experimentally observed conformer of **2A** in the solid state.

Energetics. From the total energies and zero-point-energy (ZPE) corrections, reported in Table 3SM (Supporting Information), one can obtain the relative energies of the conformers.

(12) (a) Vosko, S. H.; Wilk, L.; Nusair, M *Can. J. Phys.* **1980**, *58*, 1200. (b) Becke A. D. *Phys. Rev. A* **1988**, *38*, 3098. (c) Lee, C.; Yang, W.; Parr, R. G. *Phys. Rev. B* **1988**, *37*, 785. (d) Miehlich, B.; Savin, A.; Stoll, H.; Preuss, H. *Chem. Phys. Lett.* **1989**, *157*, 200. (e) Becke, A. D. *J. Chem. Phys.* **1993**, *98*, 5648. (f) Godbout, N.; Salahub, D. R.; Andzelm, J.; Wimmer, E. *Can. J. Chem.* **1992**, *70*, 560.

Table 5. Relative Energies of the **2A** and **2B** Adducts, Including the ZPE Correction, with Respect to the Most Stable Conformer Obtained for Different E_{XC} Energy Functionals and Basis Sets[a]

adducts	LDA DZVP	BLYP DZVP	B3LYP DZVP	B3LYP DZVP2	B3LYP 6-31+G(d,p)
2A−T_1	3.1 (3.4)	2.0 (2.1)	2.3 (2.5)	2.2 (2.4)	2.0 (2.2)
2A−T_2	0 (0)	0 (0)	0 (0)	0 (0)	0 (0)
2B	6.0 (6.6)	4.9 (5.4)	5.2 (5.6)	5.4 (6.0)	4.9 (5.4)

[a] The values in parenthesis are the relative energies without the ZPE correction. All quantities are in kcal/mol.

Table 6. Relative Energies without ($-\Delta E$) and with ZPE Corrections ($-\Delta E^{ZPE}$) of the Isomeric and Conformational Forms of **1**−**3** and Their Dipole Moments (μ), Calculated on the B3LYP/6-31+G(d,p) Level[a]

adducts	$-\Delta E^{ZPE}$	μ
1A−T-1	1.9	3.4
1A−T-2	0	1.1
1B[b]	3.3	6.9
2A−T-1	2.0	4.0
2A−T-2	0	0.9
2B[b]	4.9	8.4
3A−T-1	1.9	3.9
3A−T-2	0	2.3
3B−T-1[c]	4.6	7.8
3B−T-2[d]	3.9	7.7

[a] Energies are in kcal/mol, and dipole moments are in debye. [b] According to calculations, the cis adduct also has a twist conformation. [c] The $C(5)H_2$ protons are closer to BF_3. [c] The $C(5)H_2$ protons are closer to BH_3.

These results for different E_{XC} functionals and basis sets are presented in Table 5. It should be first noted that, irrespective of the E_{XC} functional and basis set, all theoretical levels predict the same conformational ordering, namely, **2A**−**T2** < **2A**−**T1** < **2B**.

Second, LDA shows an overestimation of ≈1 kcal/mol in the conformational energy differences, but the GGA and hybrid approaches have a difference of 0.3 kcal/mol. The ZPE produces changes in the relative energies of 0.6 kcal/mol for the cis−trans compounds and 0.3 kcal/mol in the energy difference between two twisted trans conformers. The conformational energy differences are also quite stable with respect to the choice of basis sets; polarization functions in the hydrogen atoms have an effect of 0.1−0.2 kcal/mol, and diffuse functions tend to reduce these energy differences by no more 0.5 kcal/mol. In summary, one can safely conclude that the conformational energy differences of adducts, like those studied in this work, are well-represented by the GGA and hybrid exchange-correlation energy functionals with double-ζ plus polarization functions basis sets.

Taking into account the above conclusions, a search on the PES of structures **1**−**3** was performed with the hybrid functional B3LYP and the 6-31+G(d,p) basis set, which was selected to describe properly the potential weak interactions in these isomers.

Relative energies of the structures for trans and cis adducts are compared in Table 6. It is seen that cis locations of two BH_3, BF_3, or BH_3/BF_3 groups lead, in all cases, to an increase of total energies.

Conformations **T-1** were experimentally established for **1A** and **2A** in the solid state and in solutions. In contrast, the computation of **1**−**3** (gas phase) reveals that the twisted conformers **T-2** (Chart 2) are the lowest lying conformers on the PES (Table 6). It should be emphasized that the energy differences between **T-1** and **T-2** do not change dramatically with the use of polarization functions and ZPE corrections.

Table 7. Results of the AIM Analysis for Adducts 1 and 2: The Value of the Electronic Density (ρ_C), the Laplacian of the Density ($\nabla^2\rho_C$) and the Ellipticity (ϵ_C) Calculated at the Corresponding Critical Points (see Figure 3)[a]

adduct	bond[b]	ρ	$\nabla^{2\rho}$	ϵ
1A−T-1	$H_2C-H\cdots HBH_2$ (1)	0.0079	0.0220	0.0807
1A−T-2	$H_2C-H\cdots HBH_2$ (1)	0.0054	0.0166	0.4283
	$HC-H\cdots HBH_2$ (1)	0.0102	0.0371	2.0413
1B	$H_2C-H\cdots HCH_2$ (1)	0.0068	0.0247	0.1855
2A−T-1	$H_2C-H\cdots FBF_2$ (1)	0.0080	0.033	0.0434
2A−T-2	$H_2C-H\cdots FBF_2$ (2)	0.0045	0.0202	1.6442
	$HC-H\cdots FBF_2$ (2)	0.0120	0.0506	0.3388
2B	$H_2C-H\cdots HCH_2$ (1)	0.0071	0.0260	0.1598

[a] All quantities are in atomic units. [b] Number of bonds.

Finally, the computation also shows an important feature of the **T-2** structures: they possess the smallest dipole moments (Table 6).

Topological Analysis of the Electron Density. To analyze the bonding in the amineboranes, the critical points (bond, ring, and cage), CPs, and the gradient paths of structures **1**, **2,** and **3** were calculated. To characterize the nature of the proton−hydride and proton−fluoride interactions, the density, Laplacian and ellipticity (bond descriptors) of the CPs were also obtained. This analysis was performed using the density matrix obtained from Gaussian for a B3LYP/6-31+G(d,p) calculation of each structure that was fed to Bader's AIMPAC program package[12a] to obtain the CPs and bond descriptors. The choice of basis sets follows from the discussion in the previous subsection and is dictated by the fact that diffuse functions are important for the correct description of weak interactions.

Results of the topological analysis of **1** and **2**, obtained with B3LYP/6-31+G(d,p), are presented in Table 7, and the molecular graphs of adduct **2A** are depicted in Figure 3.

Both twisted conformations of **1A** and **2A** show critical points along directions CH···FB and CH···HB, and the values of the descriptors allow us to classify these CPs as closed-shell interactions.[11a] It is worth noting that some values of the electron densities at these CPs are quite small. For example, for the CPs along CH···HB in **1,** the electronic density is lying in the range 0.005−0.0102 au, which is close, but with the lower limit smaller than those reported for dihydrogen bonds $H_3CH\cdots HF$ and $H_3SiH\cdots HF$.[3c]

Finally, all **T-1** structures have only one bond critical point that can be attributed to a H···H or H···F bond. In the **T-2** conformers there are at least two gradient paths that can be interpreted as weak closed-shell interactions. It is important to note that because the distances between these CPs and their closest ring CP are small, one can predict that even small molecular deformations will result in the disappearance of some of these paths. Actually, the NMR data do not show such nonsymmetry in solutions.

Discussion

The experimental studies of the borane adducts can be summarized as follows: (a) bis(BH_3) adduct **1** prefers trans structure **1A** with a trans/cis isomeric ratio of 9:1. (b) *Cis*-BF_3/BF_3 and BH_3/BF_3 adducts (**2B**, **3B**) were unobservable in the NMR spectra. (c) Bis adducts **1A** and **2A** have in solutions a frozen **T-1** conformation in which both methylene $N(1)CH_2$-$CH_2N(3)$ protons are oriented toward BH_3 or BF_3 (Chart 2). (d) Solid **2A** exists as twist conformation **T-1**. (e) The BH_3 and BF_3 groups modify strongly the ^1H NMR parameters of the cycles.

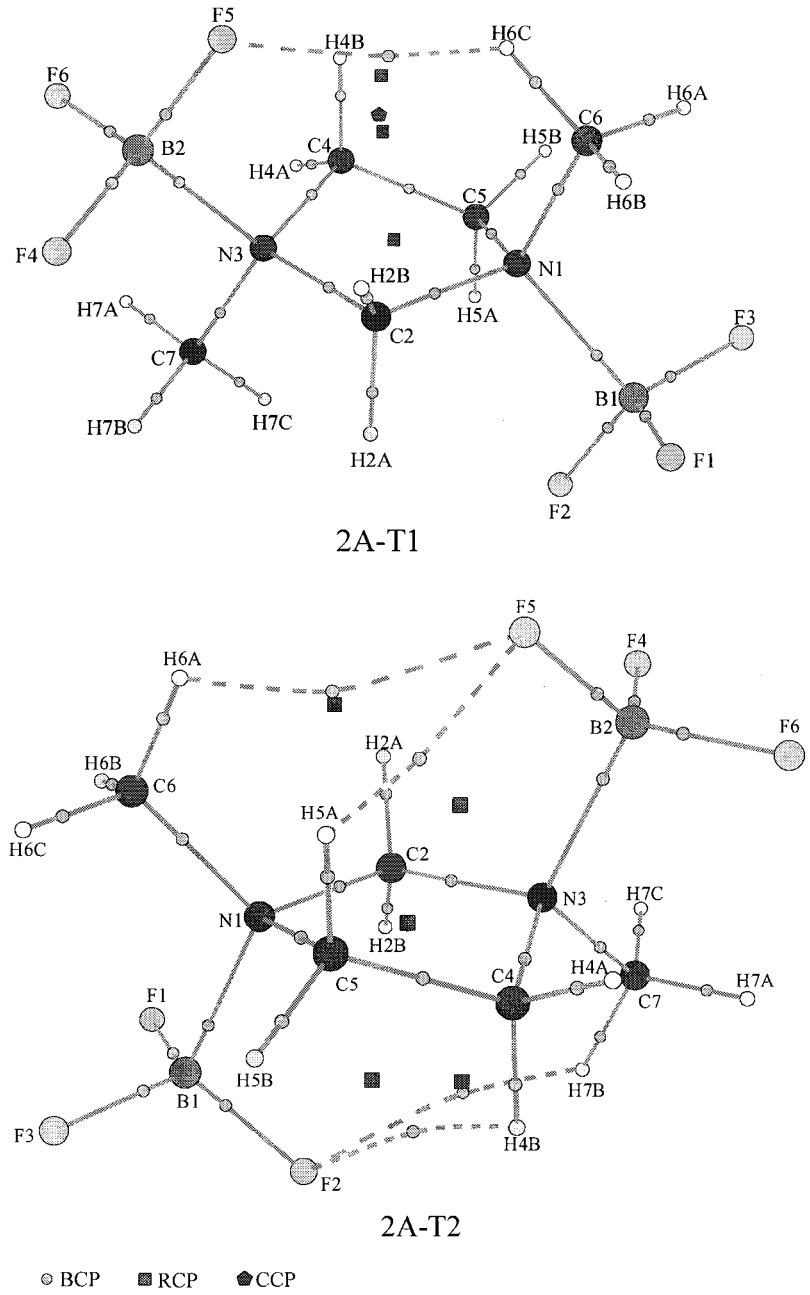

Figure 3. Molecular graphs corresponding to adducts **2A**−**T1** and **2A**−**T2** obtained with B3LYP and 6-31G+(d,p) basis.

Formally, these data support the idea about the existence of proton−hydride or proton−fluoride interactions, operating even at long distances and stabilizing conformational states. Moreover, we have found that the *J* parameters of the AA′BB′ system of protons 5, 5′, 4 and 4′ in a benzene solution of **1A** do not change, even in the presence of an excess of MeOH, provoking the formation of intermolecular $OH^{\delta+}\cdots{}^{-\delta}HB$ hydrogen bonds.[2b] Finally, the topological analysis of **T-1** and **T-2** actually demonstrates the presence of bond critical points in the expected directions.

However, consider the computed relative energies of the **T-1** structures for trans and cis isomers. Table 6 shows that **1B** is less stable than **1A** by 1.4 kcal/mol (including ZPE). According to Bolzmann's distribution, this conformational energy difference reasonably reproduces the isomeric ratio determined experimentally. The calculated stability of trans adducts **2A** and **3A** is more pronounced: their ΔE values reach 2.9 and 2.7 kcal/mol, respectively. Note that cis adducts **2B** and **3B** were unobservable in the NMR spectra of reaction solutions, and thus, the computation again agrees with the experiments.

Simple geometrical considerations show that the twist conformations minimize spatial (repulsive) interactions between the bulky groups. In this context, it is interesting that in cis **2B**, the theoretical values of the H···H (between two neighboring CH_3 groups) and F···F (between two BF_3 groups) contacts are equal to 2.26 and 3.75 Å, respectively. It is remarkable that the F···F distance is significantly larger than the sum of the van der Waals radii of F ($r_{VDW}(F) = 1.5-1.6$ Å), and the H···H contact is even shorter than 2.4 Å. This is a good illustration of a strong BF_3/BF_3 repulsion (with respect to interactions CH_3/CH_3) that destabilizes the cis adduct. Probably, the BF_3/BF_3 repulsion causes a spatial approach of the methyl groups and, consequently, the appearance of the corresponding critical point with the very low electronic density ($\rho_C = 0.0071$ and $\nabla^2_{\rho C} = 0.026$). Finally, the ΔE values in Table 6 show the following energetic preference of trans adducts: **2A** (2.9 kcal/mol) > **3A** (2.7 kcal/

mol) > **1A** (1.4 kcal/mol). This order is in line with the expected increase in the spatial extent of the groups: $CH_3 < BH_3 < BF_3$. Hence, the isomeric ordering of the investigated compounds is dictated by spatially repulsive interactions.

According to the DFT calculations, adducts **1**−**3** prefer conformations **T-2** in the gas phase. It is interesting that the relative energies (ΔE^{ZPE}) between the **T-2** and **T-1** conformers are practically identical for all of the adducts, that is, $\Delta E^{ZPE} =$ 1.9−2.0 kcal/mol (Table 6). In contrast to **T-1**, structures **T-2** show two (or more) bond critical points that connect the corresponding atoms. It is reasonable to assume that this fact elucidates the origin of the **T-2** stabilization. In such case, and on the basis of the relative energies and the topological analysis of the electric density, one can crudely estimate the energy of one proton−hydride and one proton−fluoride contact as 1.9 (**1A**−**T2**) and 0.7 (**2A**−**T2**) kcal/mol, respectively. Note that this estimation is in a reasonable agreement with ab initio studies of H-bonded complex SiH_4···HF, where the H···H distance and the $-\Delta H°$ value are calculated as 2.0 Å and 0.9−0.7 kcal/mol, respectively.[3c] Hence the elongated intramolecular interactions $CH^{\delta+}\cdots{}^{-\delta}$HB and $CH^{\delta+}\cdots{}^{-\delta}$FB studied in the present work can be classified as weak ones. Nevertheless, twist-conformations **T-2** are stabilized in the gas phase, namely, by proton−hydride or proton−fluoride interactions. The experimentally observed **T-1** structure in a condensed phase (solution or solid) can be rationalized taking into account the big difference between the dipole moments of conformers **T-1** and **T-2** (see Table 6). In a condensed phase, the initial aggregation is dominated by the long-range electrostatic interaction. The stronger dipole−dipole interaction of a pair, **T-1**−**T-1** or **T-1**−solvent, as compared with a **T-2**− **T-2** pair or **T-2**−solvent, will drive the system to a preferential **T-1** state instead of the stable **T-2** conformational state in the gas phase. Finally, it should be emphasized that despite a weakness of the elongated proton−hydride and proton−fluoride interactions, with an estimated upper limit of 2 kcal/mol, they can dictate conformational molecular states especially in the case of their cooperative actions.

Conclusions

The structures of bis(BH_3), -BF_3 and -NBF_3/BH_3 adducts **1**−**3** have been characterized by the multinuclear NMR spectra, the X-ray data (adduct **2**) and the DFT calculations at different theoretical levels. It was shown that the hybrid approach B3LYP with any of the basis used in this work is a reasonable chemical model to study the molecular structure of amineboranes.

The experimental and theoretical data have shown that bis adducts **1**−**3** prefer trans orientations of the borane groups in solutions, the solid state, and the gas phase. The energetic preference of trans adducts, **2A** (2.9 kcal/mol) > **3A** (2.7 kcal/mol) > **1A** (1.4 kcal/mol), is dictated by spatially repulsive interactions.

The DFT calculations and the topological analysis of electronic densities have revealed that trans adducts **1**−**3** exist in the gas phase as twist conformations **T-2**, which are stabilized by the intramolecular $C-H^{\delta+}\cdots{}^{-\delta}H-B$ or $C-H^{\delta+}\cdots{}^{-\delta}F-B$ bonding. These interactions are characterized as weak and closed-shell because ρ_C are small and the $\nabla^2_{\rho C}$ values are positive. The energy of one proton−hydride and proton−fluoride contact is estimated as 1.9 (**1A**−**T2**) and 0.7 (**2A**−**T2**) kcal/mol, respectively, and hence, the intramolecular interactions $CH^{\delta+}\cdots{}^{-\delta}$HB and $CH^{\delta+}\cdots{}^{-\delta}$FB studied in the present work can be classified as weak ones.

The experimental and theoretical information shows that, on going from the gas phase to a condensed phase (solution and solid), the twist conformations **T-2** transform to conformations **T-1**, probably by intermolecular dipole−dipole interactions.

The data gathered in this work demonstrate that despite a weakness of the proton−hydride and proton−fluoride interactions, they can play a significant role in the stabilization of conformational molecular states,especially when cooperativity is involved.

Experimental Section

The NMR spectra were obtained with JEOL GXS-270, JEOL-400, and Bruker-300 spectrometers. The ^{1}H and ^{13}C NMR spectra were referred to TMS. The T_1 measurements were carried out by the standard inversion−recovery (180° − τ − 90°) method with a Bruker 300 NMR spectrometer in deoxygenated solutions. The calculation of the relaxation times was made using the nonlinear three-parameter fitting routine of the spectrometer. In each experiment, the waiting period was 5 times longer than the expected relaxation time, and 16 variable delays were employed. The T_1 determinations were carried out with errors ≈5%.

The X-ray diffraction studies were performed with a Siemens P4 instrument equipped with a CCD area detector and a low-temperature device LT2 using MoKα radiation and graphite monochromator. Data were collected in the hemisphere mode. Structure solution and refinement were performed using the program SHELXL-97. Crystallographic data have been deposited at the Cambridge Crystallographic Data Center and allocated the deposition number CCDC-162617. Copies of the data can be received free of charge on application to CCDC, 12 Union Road, Cambridge CB2 1EZ, U.K. [Fax: int. code + 44-1223/336-033; E-mail:deposit@ccdc.cam.ac.uk].

All of the solvents and amines were freshly distilled and dried before use according to convenient procedures.

1,3-Dimethyl-1,3-diazolidine (4). The compound was prepared by the method[13] using the *N*,*N*-dimethylethylenediamine and formaldehyde in CH_2Cl_2 as azeotropic agent. The reaction mixture was refluxed for 8 h, and then the solvent was evaporated. The final product was purified by distillation in a vacuum and kept in nitrogen atmosphere. ^{1}H NMR ($CDCl_3$): δ = 3.58 (s, 2, 2′); 2.81 (s, 4, 4′, 5, 5′); 2.41 (s, CH_3).

***N*-BH_3 and N−BF_3 Bis Adducts 1, 2.** Preparation of the compounds was carried out by an addition of 1.2 or 2 equiv of BH_3·THF (1.31 M) or BF_3·OEt_3 solutions to 1 equiv of dry amine **4** in 5 mL of THF at room temperature and under anhydrous conditions. The yields were quantitative. The excess of BH_3·THF was evaporated under a high vacuum. The compounds were kept under a nitrogen atmosphere.

***N*-BH_3−*N*-BF_3 Adduct 3.** The product was prepared by an addition of 1 equiv of BH_3·THF to 1 equiv of dry amine **4** in 4 mL of THF; after evaporation of THF, one 1 equiv of BF_3·OEt_3 was added. The product was obtained as a mixture with **1A** and **2A** and characterized by the ^{1}H and ^{13}C NMR spectra.

Compound 1A. ^{1}H NMR ($CDCl_3$): δ = 4.08 (s, 2, 2′); 3.57 (s, 4, 4′, 5, 5′); 2.93 (s, CH_3); 1.85 (bqv, BH_3). ^{13}C NMR ($CDCl_3$): δ = 89.2 (t, C-2, ^1J(C−H) = 160.2 Hz); 61.2 (t, C-4 (5), ^1J(C−H) = 148.7 Hz); 53.3 (q, CH_3, ^1J(C−H) = 141.8 Hz). ^{11}B NMR ($CDCl_3$): δ = −8.5 (q, BH_3, ^1J(B−H) = 98 Hz).

Compound 1B. ^{1}H NMR ($CDCl_3$): see Table 1 and δ = 2.93 (s, CH_3); 1.8 (bqv, BH_3). ^{13}C{^{1}H} NMR ($CDCl_3$): δ = 89.2 (C-2), 60.8 (C-4 (5)), 52.5 (CH_3).

Compound 2A. ^{1}H NMR ($CDCl_3$): see Table 1 and δ = 2.90 (bs, CH_3); 1.8. ^{13}C NMR ($CDCl_3$): δ = 78.1 (t, C-2, ^1J(C−H) = 159.6 Hz); 55.7 (t, C-4 (5), ^1J(C−H) = 152.6 Hz); 45.7 (q, CH_3, ^1J(C−H) = 143.0 Hz). ^{11}B NMR ($CDCl_3$): δ = −0.6 (q, BF_3, ^1J(B−F) = 15.2 Hz).^{19}F NMR ($CDCl_3$): δ = −160.5.

Compound 3A. ^{1}H NMR ($CDCl_3$): δ = 4.01 and 4.24 (d, 2, 2′, ^2J(2−2′) = 7.8 Hz); 3.30 and 3.27 (m, 5, 5′); 3.52 and 3.55 (m, 4, 4′); 2.97 (s, CH_3N(1)); 2.83 (s, CH_3N(3)); 1.6 (bqv, BH_3). ^{13}C NMR ($CDCl_3$): δ = 83.2 (t, C-2, ^1J(C−H) = 158.4 Hz); 61.0 (t, C-4, ^1J(C−H) = 149.1 Hz); 55.4 (t, C-5, ^1J(C−H) = 152.2 Hz); 46.8 (q, Me-N1,

(13) (a) Chapuis, C.; Gauvreau, A.; Klaebe, A.; Lattes, A.; Perie, J. J.; Roussel, J. *Tetrahedron* **1974**, *30*, 1383. (b) Anet, F. A. L.; Yavari, I. *Org. Magn. Reson.* **1979**, *12*, 362. (c) Fülöp, F.; Bernath, G.; Marttinen, J.; Pihlaja, K. *Tetrahedron* **1989**, *45*, 4317.

^1J(C−H) = 142.0 Hz); 52.1 (q, Me-N3, ^1J(C−H) = 141.4 Hz). ^{11}B NMR ($CDCl_3$): $\delta = -8.7$ (q, BH_3, ^1J(B−H) = 95 Hz); 0 (q, BF_3, ^1J(B−F) = 13.1 Hz);.^{19}F NMR ($CDCl_3$): $\delta = -161.2$.

Acknowledgment. V.I.B. thanks Conacyt-Mexico for a Catedra Patrimonial, and M.G.-R. and G.M., for a scholarship and grant no. G32-710-E from Conacyt. Financial support from Cinvestav is acknowledged.

Supporting Information Available: Tables giving crystal data, structure refinement details, atomic coordinates, bond lengths, and angles for **2A**. Tables providing the computed structural information for **1**-**3**. This material is available free of charge via the Internet at http://pubs.acs.org.

JA0111232